Multi-muscle functional electrical stimulation based wrist tremor suppression using repetitive control

Zan Zhang, Bing Chu,Yanhong Liu, Zhe Li and David H Owens

***Abstract*—Wrist motion is produced by a group of muscles acting in a coordinated way. However, existing functional electrical stimulation based wrist tremor suppression methods just stimulate one pair of muscles, which can limit the tremor suppression performance and cause muscle fatigue. To address these problems, this paper proposes a multi-muscle FES-based wrist tremor suppression method by fully considering the properties of wrist motion. First, with consideration of the mainly involved two pairs of muscles in wrist flexion and extension motion, a multi-muscle wrist musculoskeletal model with Hammerstein structure is developed and the parameters are identified. Then, a feedback repetitive controller combined with a feed-forward linearization controller is proposed for tremor suppression. Frequency modified inverse repetitive control algorithm and gradient-based repetitive control algorithm are put forward to regulate the FES level properly. Finally, experiments on both unimpaired subjects and intention tremor patients verify that compared to the existing single muscle pair FES based methods, the proposed methods can substantially improve the performance of tremor suppression and effectively reduce the level of electrical stimulation significantly, thereby reducing muscle fatigue.**

***Index Terms*—Wrist tremor suppression, multi-muscle functional electrical stimulation, musculoskeletal model, repetitive control, experimental verification**

I. Introduction

INTENTION tremor is one of the common symptoms of cerebellar diseases, such as diffuse axonal injury, multiple sclerosis, etc. [1]. It usually occurs during goal-directed movements and the tremor amplitude increases as the target is approached [2]. So the precise arm and hand movements are impossible for intention tremor patients, which seriously affects their quality of life, such as eating, dressing and writing.

A number of methods have been proposed for tremor suppression. Prescription medication is a traditional therapy, which however often causes side effects, such as 'off episodes' [3]. Invasive surgical treatments, such as stereotactic thalamotomy [4], stereotactic pallidotomy [5] and deep brain stimulation [6], have inherent risks and the cost of the surgery is expensive. Assistive treatments, such as biomechanical loading [7], limb cooling [8] and tremor suppression exoskeleton [9, 10] may cause clumsiness and slowness in performing tasks. As an alternative, functional electrical stimulation (FES) is shown promising due to its minor side effects, low-cost and portability [11, 12, 13, 14, 15].

FES uses electrical pulses to stimulate the related muscles to restore the motor functions [16]. FES based wrist tremor suppression is achieved by generating anti-phase electrical pulses with respect to tremble motion so as to reduce the resulting movement caused by tremor. A number of FES based feedback control systems were proposed to suppress tremor motion by adjusting the appropriate level of FES signals. A filter-based controller was first developed in [11, 17] and tremor patients participated in the study to confirm the feasibility of FES-based tremor suppression. Extended Kalman filter based control [12], PI control [13], neural oscillator control [14] and repetitive control (RC) [15] were also applied to improve the performance of FES based tremor suppression.

Although the above designs have been shown promising for FES based tremor suppression, they all use only one pair of muscles. However, even for single degree of freedom of wrist movement, such as wrist flexion and extension motion, there are at least two pairs of muscles involved [18]. Just stimulating one pair of muscles inevitably limits the performance of tremor suppression. Moreover, it also requires a higher level of electrical stimulation signal contributing to muscle fatigue, which is undesirable and a key factor preventing the successful use of FES in practice [19].

To address above limitations, this paper proposes an FES based tremor suppression method stimulating multiple pairs of muscles. The main contributions of the paper can be summarized as follows:

(1) The development of a multiple muscle pair musculoskeletal dynamic model for FES based tremor suppression. The proposed model can capture the complex nature of the muscle dynamics and has a simple structure to allow an automated parameter estimation procedure that can be easily used in clinical settings.

(2) The design of a combined control scheme for tremor suppression. A feedback repetitive controller combined with a feed-forward linearizing control is constructed to suppress tremor. The asymptotical stability properties are analysed and two methods for implementing the proposed repetitive

Zan Zhang, Yanhong Liu and David H Owens are with School of Electrical Engineering, Zhengzhou University, Zhengzhou, China, (e-mail: zanzan@zzu.edu.cn, liuyh@zzu.edu.cn).

Bing Chu is with Department of Electronics and Computer Science, University of Southampton, Southampton, SO17 1BJ, UK (e-mail: B.Chu@soton.ac.uk).

Zhe Li is with the Rehabilitation Department, Fifth Affiliated Hospital of Zhengzhou University, Zhengzhou, China (e-mail: lizhe.1974@163.com).

David H Owens is also with Department of Automatic Control and Systems Engineering, The University of Sheffield, Mappin Street, Sheffield, S1 3JD, UK (e-mail:d.h.owens@sheffield.ac.uk).

This work is supported by the National Key Research and Development Project (No. 2020YFB1313701), the National Natural Science Foundation of China (No. 61803344, 62003309) and the Outstanding Foreign Scientist Support Project in Henan Province (No. GZS2019008).

Corresponding author: Yanhong Liu

controller are also presented.

(3) Experimental verification on both healthy subjects and intention tremor patients. Experimental results show that compared to existing design stimulating single muscle pair, the proposed multi-muscle FES method can substantially improve the tremor suppression performance and reduce the level of electrical stimulation significantly.

The rest of the manuscript is organized as follows: Section II gives an overview of the proposed multi-muscle FES based wrist tremor suppression system. Modeling of the multi-muscle wrist musculoskeletal dynamics are presented in Section III. Section IV proposes a combined controller design with a linearizing control and a repetitive controller. In Section V, a systematic experimental approach is designed and results are given to verify the effectiveness of the proposed method. Finally, conclusions and future work are set out in Section VI.

II. System overview

Intention tremor is a kind of kinetic tremor and usually occurs during goal-directed movements, that is, increasing in tremor amplitude as the target is approached [2]. Wrist tremor is a common symptom in patients with intention tremor [7]. It can cause uncontrollable wrist motions, and affect the fine movement of the hand, thus seriously affecting the life of patients. In this paper, we focus on the tremor suppression of wrist flexion and extension motion because this degree of freedom motion occurs frequently in the people's daily activities.

There are two pairs of extensors and flexors that play a key role in the wrist flexion and extension motion: flexor carpi radialis (FCR), extensor carpi radialis (ECR), flexor carpi ulnaris (FCU) and extensor carpi ulnaris (ECU) [18]. However, most existing FES based tremor suppression system just stimulated one pair of muscles, e.g., FCU and ECU in [13], FCU and ECR in [14], and FCR and ECR in [15], which can limit the performance of tremor suppression and accelerate the muscle fatigue. Fully considering the properties of wrist motion and related muscles, the above two pairs of muscles are used to suppress tremor in this paper. The diagram of the multiple-muscle FES based wrist tremor suppression control system is shown in Fig. 1, which mainly includes the model of the wrist musculoskeletal dynamics, the feedback controller, the electrical stimulator and the angle sensor.

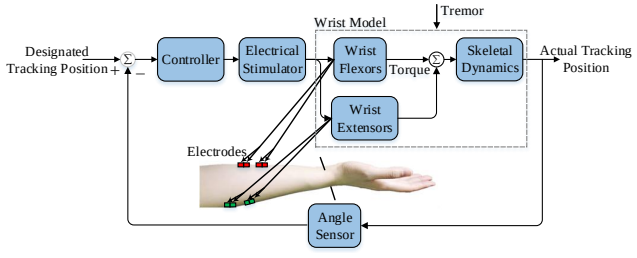

Fig. 1. The diagram of the multi-muscle FES based control system for wrist tremor suppression

Noticing that intention tremor causes uncontrollable wrist motion and hinders the precise movement, it can be regarded as an external disturbance injected into the wrist musculoskeletal system. Due to the existence of intention tremor, there will be position error between the designated tracking position (voluntary motion) and the actual tracking position. In the experimental tests, the designated voluntary tracking position is the reference position given to the subjects (for them to track). This reference resembles some of the simple daily tasks, e.g., moving the hand to reach a particular angle. The designated tracking position is not estimated, but set in advance in the experimental tests. To minimize the position error, a feedback controller will be designed to make the electrical stimulator generate multi-channel stimulation signals. The electrical stimulation level needs to be properly adjusted by the feedback controller. The multi-channel FES signals are then applied to the wrist flexors and extensors through the electrodes to contract the corresponding muscles and generate an anti-phase torque to suppress the wrist tremor.

III. Modeling of wrist musculoskeletal dynamics

In order to design a controller to regulate the FES levels, a model of the wrist musculoskeletal dynamics need to be established first. In this section, we will develop a Hammerstein structure model of multiple muscle pairs musculoskeletal dynamics.

A. Structure of wrist musculoskeletal dynamic model

The sketch of the main muscles and skeletons related to the wrist flexion and extension motion is shown in Fig. 2, where FCR and FCU contribute to the flexion motion while ECR and ECU contribute to the extension motion. The radius and ulna are the related skeletons.

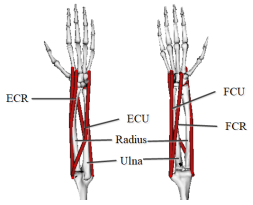

Fig. 2. The sketch of the main muscles and skeletons involved in wrist flexion and extension motion [20]

The wrist musculoskeletal dynamics consists of muscle model and skeletal model. Hammerstein model is widely used in FES based muscle modelling due to its simple structure and suitability for tremor suppression controller design [21, 22]. The Hammerstein model consists of a static nonlinear recruitment characteristics to present muscle activation property and a linear dynamic model to present the muscle contraction response to electrical stimulation signals. The skeletal dynamics of human limbs can be modeled as rigid body dynamics (RBD).

The structure of the musculoskeletal model is shown in Fig. 3, where the input $u_j(k)$ ($j = \mathrm{fcr}, \mathrm{ecr}, \mathrm{fcu}, \mathrm{ecu}$) is the non-negative electrical stimulation signal; $f_j(u_j)$ presents the nonlinear static recruitment characteristic of FCR, ECR, FCU and ECU respectively; $w_j(k)$ is the steady-state isometric muscle torque; $G_j(z)$ is the linear contraction dynamics of the four main involved muscles; $\tau_j(k)$ is the torque generated by the muscles and $\tau(k) = \tau_{\mathrm{fcr}}(k) - \tau_{\mathrm{ecr}}(k) + \tau_{\mathrm{fcu}}(k) - \tau_{\mathrm{ecu}}(k)$

is the total torque acting on the skeletal system; $G_{RBD}(z)$ presents the skeletal dynamics of the wrist; the output $y(k)$ is the angle of wrist joint motion; the antagonist and agonist muscle pairs have input from the same oscillatory source at the tremor frequency [23]. Therefore, $d(k)$ is regarded as the equivalent disturbance generated by tremor torque in the system, which leads to the angle deviation.

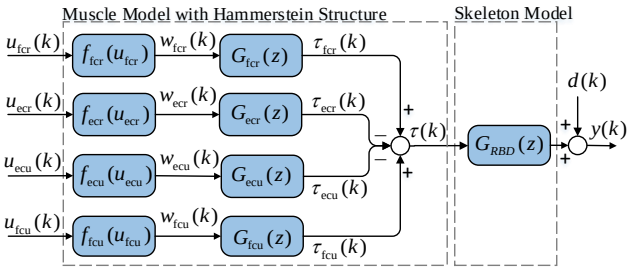

Fig. 3. The wrist musculoskeletal model with Hammerstein structure

B. Modelling of static nonlinearity and simplification

The static recruitment characteristic of Hammerstein model, or the so-called isometric recruitment curves (IRCs), presents the relationship between the electrical stimulation signal and the output torque of the corresponding muscles. A typical isometric recruitment curve includes the initial dead-zone region, the high-slope (monotonically increasing) region and the saturation region [24]. The typical IRCs of radial muscles are shown in Fig.4 (a), where $u_{\mathrm{fcr,zo}}$ and $u_{\mathrm{ecr,zo}}$ are the dead zone values of the IRCs.

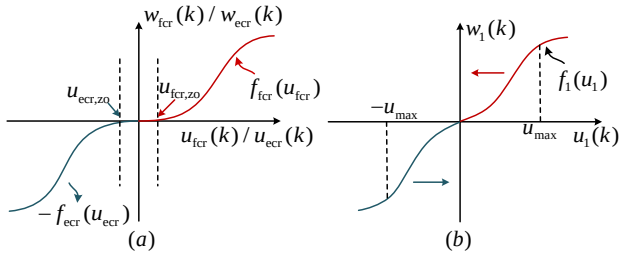

Fig. 4. (a) Typical IRCs of radial muscles. (b) Modified IRC of radial muscles.

In order to simplify the model structure and the corresponding parameter identification procedure, the $u_{\mathrm{fcr}}(k)$ and $u_{\mathrm{ecr}}(k)$ can be compacted to a new control input $u_1(k)$ to generate radial flexion and extension movement (as only one of the above two muscles is stimulated at a time). Let

$$u_{\mathrm{fcr}}(k) = \begin{cases} u_1(k) + u_{\mathrm{fcr,zo}}, & u_1(k) \geq 0, \\ 0, & u_1(k) < 0, \end{cases} \tag{1}$$

$$u_{\mathrm{ecr}}(k) = \begin{cases} 0, & u_1(k) \geq 0, \\ u_{\mathrm{ecr,zo}} - u_1(k), & u_1(k) < 0, \end{cases} \tag{2}$$

then the dead zones of the radial muscles IRCs can be removed, as shown in Fig. 4(b), where $u_{\max}$ is the saturation value of IRCs.

The IRCs of radial and ulnar muscles are similar under the same electrical stimulation inputs [25]. Therefore, the electrical stimulation inputs of ulnar muscles can also be formulated as a single $u_2(k)$ input as follows

$$u_{\mathrm{fcu}}(k) = \begin{cases} u_2(k) + u_{\mathrm{fcu,zo}}, & u_2(k) \geq 0, \\ 0, & u_2(k) < 0, \end{cases} \tag{3}$$

$$u_{\mathrm{ecu}}(k) = \begin{cases} 0, & u_2(k) \geq 0, \\ u_{\mathrm{ecu,zo}} - u_2(k), & u_2(k) < 0, \end{cases} \tag{4}$$

where $u_{\mathrm{fcu,zo}}$ and $u_{\mathrm{ecu,zo}}$ are the dead zone values of ulnar muscles IRCs. In this paper, all the dead zone values are estimated by experiments and chosen as $50\mu s$.

When the electrical stimulation inputs $u_1(k)$ and $u_2(k)$ are greater than the maximum, the steady-state isometric muscle torques will not increase, that is, IRCs enter into the saturation zone. In this paper, the maximum pulse width ($u_{\max}$) of the input stimulation signals are set to $300\mu s$ to avoid uncomfortable muscle contraction [26]. In the working region of the nonlinear IRCs, the equivalent nonlinear mapping function $f_1(u_1)$ is continuous and monotonic increasing, as shown in Fig. 4(b) and can be represented as

$$f_1(u_1(k)) = \begin{cases} f_{\mathrm{fcr}}(u_1(k) + u_{\mathrm{fcr,zo}}), \\ \quad u_1(k) \in [0, u_{\max} - u_{\mathrm{fcr,zo}}], \\ -f_{\mathrm{ecr}}(u_{\mathrm{ecr,zo}} - u_1(k)), \\ \quad u_1(k) \in [u_{\mathrm{ecr,zo}} - u_{\max}, 0). \end{cases} \tag{5}$$

So does the equivalent ulnar nonlinear isometric recruitment curve $f_2(u_2)$.

C. Modelling of linear dynamics and simplification

According to [27, 28, 29], the two radial muscles FCR and ECR have similar biophysical properties, as well as the two ulnar muscles FCU and ECU, that is, $G_{\mathrm{fcr}}(z) \approx G_{\mathrm{ecr}}(z)$, $G_{\mathrm{fcu}}(z) \approx G_{\mathrm{ecu}}(z)$. Therefore, we denote the linear contraction dynamics of radius muscles FCR/ECR and ulnar muscles FCU/ECU as $G_{\mathrm{LCD1}}(z)$ and $G_{\mathrm{LCD2}}(z)$ respectively. The skeletal dynamics of human limbs can be modeled as rigid body dynamics $G_{\mathrm{RBD}}(z)$, in which the damping and elastic functions are linear.

The overall linear musculoskeletal dynamics including the linear muscle dynamics and skeletal dynamics can be modelled as $G(z) = [G_1(z) \;\; G_2(z)]$, where $G_1(z) = G_{\mathrm{LCD1}}(z)G_{\mathrm{RBD}}(z)$ and $G_2(z) = G_{\mathrm{LCD2}}(z)G_{\mathrm{RBD}}(z)$ are the equivalent linear radial and ulnar musculoskeletal dynamics respectively. Integrating the equivalent static recruitment characteristic ($f_1(u_1)$ and $f_2(u_2)$) and the linear dynamics ($G_1(z)$ and $G_2(z)$), the wrist musculoskeletal dynamics can be modelled as a two-input single-output system shown in Fig. 5, where $w_1(k)$ and $w_2(k)$ are the equivalent isometric muscle torques generated by the radial and ulnar pair of muscles.

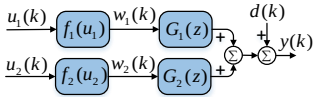

Fig. 5. The wrist musculoskeletal model with Hammerstein structure

D. Model parameterization

Due to the continuous and monotonic increasing characteristics of the IRCs, $f_1(u_1(k))$ and $f_2(u_2(k))$

can be reformulated as the following general polynomial form

$$f_i(u_i(k)) = r_0^i + r_1^i u_i + r_2^i u_i^2 + \cdots + r_s^i u_i^s, \quad (6)$$

with the monotonicity increasing conditions being satisfied

$$\frac{df_i(u_i(k))}{du_i} = r_1^i + 2r_2^i u_i + \cdots + s r_s^i u_i^{s-1} > 0, \quad (7)$$

where s is the order of the nonlinear recruitment curve and $r_0^i, r_1^i, \cdots, r_s^i$ (i=1,2) are the parameters to be identified.

The linear musculoskeletal model can be written as

$$G_i(z) = \frac{B_i(z^{-1})}{A_i(z^{-1})} = \frac{b_{i1}z^{-1} + ... + b_{in_b}z^{-n_b}}{1 + a_{i1}z^{-1} + ... + a_{in_a}z^{-n_a}}, \quad (8)$$

where n_a, n_b are the orders of $A_i(z^{-1})$ and $B_i(z^{-1})$ respectively, $a_{i1}, \cdots, a_{in_a}$ and $b_{i1}, \cdots, b_{in_b}$ (i=1,2) are parameters to be estimated. The identification of the nonlinear and linear parameters will be discussed in Section V.

IV. Tremor suppression controller design

The wrist musculoskeletal model proposed in previous section is nonlinear because of the inherent nonlinearity of the recruitment characteristics. In this section, a linearizing controller is designed first to linearize the system. Then a multiple input single output repetitive controller is developed to suppress tremor and improve the tracking performance of the wrist.

The structure of the closed-loop control system is described in Fig. 6, where $e(k)$ is the error between the designated voluntary tracking position $r(k)$ and the real time wrist angle $y(k)$. $C(z)$ is the linear repetitive controller with gains K_1, K_2 and the compensators $H_1(z)$, $H_2(z)$ to be determined later. $G_{\rm IM}$ is the transfer function of the internal model. $\bar{w}_1$ and $\bar{w}_2$ are the outputs of the repetitive controller. $g_1(\bar{w}_1)$ and $g_2(\bar{w}_2)$ are the linearizing controllers.

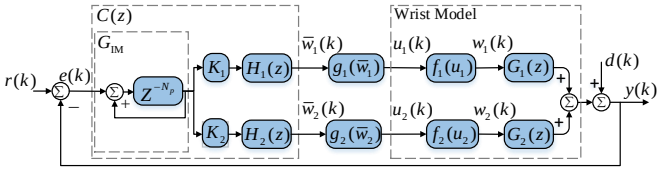

Fig. 6. Closed-loop control system structure

A. Linearizing controller design

Noticing that the equivalent static recruitment characteristics $f_1(u_1)$ and $f_2(u_2)$ are invertible, linearizing controllers can be constructed to compensate the nonlinearity as follows

$$g_1(\bar{w}_1) = f_1^{-1}(u_1), g_2(\bar{w}_2) = f_2^{-1}(u_2). \quad (9)$$

Under the linearizing controller, we have the equivalent feedback control system shown in Fig. 7, where $w(k) = [w_1(k) \quad w_2(k)]^T$ is the isometric muscle torque and $G(z) = [G_1(z) \quad G_2(z)]$ is the linear musculoskeletal model.

B. Repetitive Controller Design

Since tremor can be assumed as a roughly periodic signal, repetitive control is very suitable for the wrist tremor

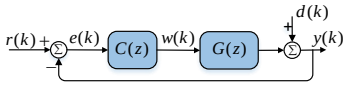

Fig. 7. The equivalent feedback RC schematic after linearization

suppression. Repetitive control is based on the internal model principle. If the repetitive controller contains a periodic signal generator, the corresponding periodic disturbance can be attenuated completely [30].

Consider the following repetitive controller

$$C(z) = [K_1H_1(z) \quad K_2H_2(z)]^T G_{\rm IM}, \quad (10)$$

where K_1, K_2 are the positive feedback gains, $H_1(z)$ and $H_2(z)$ are the compensators used to improve the stability and the dynamic performance of the closed loop system, $G_{\rm IM}$ is the internal model. The internal model can be constructed as

$$G_{\rm IM} = \frac{z^{-N_p}}{1 - z^{-N_p}}, \quad (11)$$

where $N_p = \frac{T_p}{T_s}$ is the number of samples in a period, T_p is the period of the tremor signal and T_s is the sampling period. Stability of the closed loop control system is given below.

Theorem 1. The repetitive control system shown in Fig. 6 is asymptotically stable and can completely suppress the N_p-periodic disturbance, provided that the control gains K_1, K_2 and the compensators $H_1(z)$, $H_2(z)$ satisfy the following inequalities

$$\|1 - K_1G_1(z)H_1(z) - K_2G_2(z)H_2(z)\|_\infty < 1. \quad (12)$$

Especially, when $H_1(z) = G_1^{-1}(z)$ and $H_2(z) = G_2^{-1}(z)$, the condition (12) becomes

$$0 < K_1 + K_2 < 2. \quad (13)$$

equivalently.

Proof: From Fig. 6 we can see that the relationship among the error $e(k)$, the reference $r(k)$ and the disturbance $d(k)$ can be expressed as

$$e(k) = \frac{1}{1 + G(z)C(z)}r(k) - \frac{G(z)}{1 + G(z)C(z)}d(k). \quad (14)$$

Substituting (10) into (14), we have

$$\{1 + G(z)[K_1H_1(z) \quad K_2H_2(z)]^T \frac{z^{-N_p}}{1 - z^{-N_p}}\}e(k) = r(k) - G(z)d(k). \quad (15)$$

The characteristic equation of the system can be written as

$$1 + G(z)[K_1H_1(z) \quad K_2H_2(z)]^T \frac{z^{-N_p}}{1 - z^{-N_p}} = 0. \quad (16)$$

If $K_1 > 0, K_2 > 0$ and Eqn. (16) has all roots inside the unit circle, the closed loop system is asymptotically stable. Similar to [31], the system is asymptotically stable if the following condition holds

$$\|1 - G(z)[K_1H_1(z) \quad K_2H_2(z)]^T\|_\infty < 1, \quad (17)$$

or (12) holds equivalently.

When $H_1(z) = G_1(z)^{-1}$ and $H_2(z) = G_2(z)^{-1}$, the condition (12) becomes

$$|1 - (K_1 + K_2)| < 1. \tag{18}$$

Thus complete the proof. ■

Remark 1: The characteristic equation of the system (16) can be rewritten as

$$z^{N_p} e(k) = [1 - K_1 G_1(z) H_1(z) - K_2 G_2(z) H_2(z)] e(k), \quad \forall z = e^{j\omega}, \tag{19}$$

or

$$e(k + N_p) = [1 - K_1 G_1(z) H_1(z) - K_2 G_2(z) H_2(z)] e(k), \quad \forall z = e^{j\omega}. \tag{20}$$

As can be seen, the magnitude of all frequency components of the error decays from one cycle to the next and the value of $|1-(K_1 G_1(e^{j\omega}) H_1(e^{j\omega}) + K_2 G_2(e^{j\omega}) H_2(e^{j\omega}))|$ indicates how rapidly the error converges to zero with respect to the frequency ω. Especially, when $H_1(e^{j\omega}) = G_1^{-1}(e^{j\omega})$ and $H_2(e^{j\omega}) = G_2^{-1}(e^{j\omega})$, the smaller the value $|1 - (K_1 + K_2)|$ is, the faster the error converges. The error achieves the fastest convergence speed by choosing $K_1 + K_2 = 1$.

C. Two repetitive control algorithms

From previous discussion, when $H_1(z) = G_1^{-1}(z)$, $H_2(z) = G_2^{-1}(z)$ and $K_1 + K_2 = 1$, the system is not only stable, but also has the fastest error convergence rate. However, it can be challenging in practice to choose compensator satisfying $H_1(z) = G_1^{-1}(z)$ and $H_2(z) = G_2^{-1}(z)$ due to the model parameter uncertainties and the possible non-minimum phase. In this subsection, we propose two design algorithms to approximate the system inverse, that is, we apply the frequency modified inverse repetitive control (FMI-RC) [31] and the gradient-based repetitive control (GB-RC) [32] to construct the compensator $H_1(z)$ and $H_2(z)$.

1) Frequency modified inverse RC algorithm: In this case, the compensator $H_i(z)$ is represented as a high-order FIR filter,

$$H_i(z) = c_1^i z^{m-1} + c_2^i z^{m-2} + \cdots + c_m^i z^0 + \cdots + c_n^i z^{-(n-m)}, \tag{21}$$

where $i = 1, 2$ and m, n are positive integers.

The issue of stability criteria of (12) can be addressed by selecting $H_i(z)$ as an approximation of $G_i^{-1}(z)$ at a number of frequencies ω_j, through suitable choice of parameters $\mathbf{c}^i = [c_i^l \quad c_2^i \quad \cdots \quad c_n^i]^T$ in (21). This can be achieved by minimizing the following cost function

$$J_i = \sum_{j=0}^{N} [1 - G_i(e^{i\omega_j T}) H_i(e^{i\omega_j T})][1 - G_i(e^{i\omega_j T}) H_i(e^{i\omega_j T})]^*, \tag{22}$$

where ω_j is a discrete set of frequencies selected from zero to Nyquist frequency, and $(\cdot)^*$ denotes the complex conjugate.

Let $G_i(e^{(i\omega_j T)}) = M_{G_i}(\omega_j) e^{i\varphi_{G_i}(\omega_j)}$, where $M_{G_i}(\omega_j)$ and $\varphi_{G_i}(\omega_j)$ represent the magnitude and phase of $G_i(z)$, respectively. The solution $\mathbf{c}^i$ is given by

$$\mathbf{c}^i = D_i^{-1} p_i, \tag{23}$$

where

$$D_i = \sum_{j=0}^{N} M_{G_l}^2(\omega_j) \times \Theta, \tag{24}$$

$$p_i = \sum_{j=0}^{N} M_{G_l}(\omega_j) \times \begin{bmatrix} \cos((m-1)\omega_j T + \varphi_{G_l}(\omega_j)) \\ \cos((m-2)\omega_j T + \varphi_{G_i}(\omega_j)) \\ \cdots \\ \cos((m-n)\omega_j T + \varphi_{G_i}(\omega_j)) \end{bmatrix}, \tag{25}$$

with $\Theta =$

$$\begin{bmatrix} 1 & \cos(\omega_j T) & \cdots & \cos((n-1)\omega_j T) \\ \cos(\omega_j T) & 1 & \cdots & \cos((n-2)\omega_j T) \\ \vdots & \vdots & \ddots & \vdots \\ \cos((n-1)\omega_j T) & \cos((n-1)\omega_j T) & \cdots & 1 \end{bmatrix}. \tag{26}$$

It is shown in [31] that choosing a suitable m and n by minimizing the cost function (22) can make $H_1(z)$ and $H_2(z)$ approximate $G_1^{-1}(z)$ and $G_2^{-1}(z)$ more precisely.

2) Gradient-based RC algorithm: The compensators of the gradient-based repetitive control algorithm can be constructed as

$$\begin{bmatrix} H_1(z) \\ H_2(z) \end{bmatrix} = \gamma \begin{bmatrix} G_1^*(z) \\ G_2^*(z) \end{bmatrix}, \tag{27}$$

where $\gamma > 0$ is a scalar to be chosen later, $G_1^*(z)$ and $G_2^*(z)$ are the plant adjoint operator satisfying $G_1^*(z) = G_1(z^{-1})$, $G_2^*(z) = G_2(z^{-1})$. According to Theorem 1, in order to make the system stable, (12) must be satisfied, i.e.,

$$\|1 - \gamma(K_1 G_1(z) G_1^*(z) + K_2 G_2(z) G_2^*(z))\|_\infty < 1, \forall z = e^{j\omega}. \tag{28}$$

The above indicates

$$|1 - \gamma(K_1 |G_1(z)|^2 + K_2 |G_2(z)|^2)| < 1, \forall z = e^{j\omega}, \tag{29}$$

where $|G_1(z)|$ and $|G_2(z)|$ are the magnitude of $G_1(z)$ and $G_2(z)$ respectively. So the learning gain γ needs to satisfy

$$0 < K_1 |G_1(e^{j\omega})|^2 + K_2 |G_2(e^{j\omega})|^2 < \frac{2}{\gamma} \tag{30}$$

or equivalently

$$0 < \gamma < \frac{2}{K_1 |G_1(e^{j\omega})|^2 + K_2 |G_2(e^{j\omega})|^2}, \forall \omega \geq 0. \tag{31}$$

A sufficient condition of (31) is given by

$$0 < \gamma < \frac{2}{K_1 \|G_1(e^{j\omega})\|_\infty^2 + K_2 \|G_2(e^{j\omega})\|_\infty^2}. \tag{32}$$

which is easier to be used for the calculation of γ.

V. Experimental verification

In this section, an experimental platform for wrist tremor suppression is set up and systematic experiments are carried out to verify the effectiveness of the proposed method. During the experiments, four unimpaired participants (No.1 − No.4) and two intention tremor patients are recruited. The ethical approval is obtained from the Zhengzhou University, China

(No.ZZURIB2019-004). Written informed consent is given to all participants.

A. Experimental Platform

The FES-based wrist tremor suppression experimental platform is shown in Fig. 8. It is modified from a commercially available wheelchair (Yuwell H062). The parameter identification of wrist musculoskeletal model of individual participant and the verification of the proposed control algorithms are carried out on this platform.

During the experiment, four pairs of surface electrodes (the size is 4cm×4cm and the interface is 2.0mm) are attached to FCR, ECR FCU and ECU muscles of the participant. The participant sits comfortably in the wheelchair and the arm bracket is to support the right arm of the participant. The right forearm of the participant is fixed with mould which allows the wrist flexion and extension plane motion while preventing any movement of the elbow and shoulder joints. The participant's hand is placed in the middle of the U-splint, as shown in Fig. 8. The role of U-splint is only to limit the degree of freedom of wrist motion and to generate the movement of wrist in the flexion and extension plane. When the right hand of the patient is placed in the middle of the U-splint, the U-splint will vibrate according to tremor.

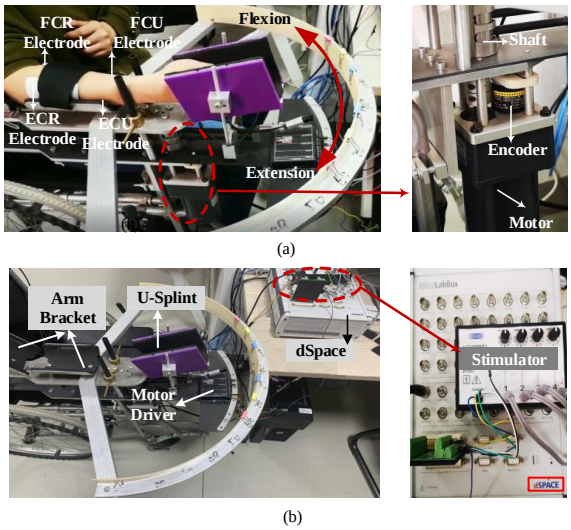

Fig. 8. The structure of experimental platform for wrist tremor suppression

The experimental platform embeds a DC-motor (BJ VDM08SGN24-60-1800/JB5G12T) which can generate artificial tremor signals. This ensures that the experiment can be carried out on the unimpaired participants. For this type of research, conducting feasibility test on healthy subjects is an essential step before clinical trials. The motor driver (ESCON50/5) is used to control the motor, as shown in Fig. 8. The torque of the DC-motor is transmitted to the purple U-shaped splint through the shaft. The tremor signal is introduced when the motor operates, and the motion will make the wrist and hand vibrate consequently. The wrist flexion and extension motion angle of the participant can be obtained by the encoder (E6B2-CWZ6C) which is mounted on the coaxial shaft of the U-shaped splint. The encoder data is collected though the real-time hardware dSpace (MicroLabBox 1202), which can interface directly with Matlab/Simulink to obtain the wrist angle data and to generate the FES signals to a four-channel electrical stimulator (Odstock Medical). The frequency, current amplitude, and maximum pulsewidth of the stimulation signal are set to 40 Hz (biphasic and asymmetrical pulse width modulation (PWM) sequences), 20 mA, and 300 μs, respectively, in this study. The amplitude of the PWM wave can be adjusted via the potentiometer of each channel on the stimulator.

B. Experimental Protocol

The experiment protocol includes two steps: parameter identification of the wrist musculoskeletal model and FES based wrist tremor suppression.

1) Parameter identification of the wrist model: The parameters identification of the wrist model is based on the input/output data set $[u, y]$. The input signals $u(k) = [u_1(k) \quad u_2(k)]^T$ are set as sine waves with different frequencies ranging from 0.2Hz to 4Hz and 300μs pulse width. $y(k)$ is the angle data of wrist flexion and extension motion measured by the encoder. Note that the motion of the participant's wrist is driven by input electrical stimulation signals during identification process. Each identification process lasts about two minutes and a validation test is conducted by reapplying the input data set for identification accuracy.

2) Wrist tremor suppression: The following two cases are carried out during the tremor suppression experiments.

Case I: Experiments on unimpaired participants by inducing tremor with single frequency;

For each unimpaired participant, the following three tests are done during Case I:

Test 1 (T1): Voluntary position tracking without induced tremor and FES.

Test 2 (T2): Voluntary position tracking with induced tremor but without FES.

Test 3 (T3): Voluntary position tracking with induced tremor and FES (5 repeated trials are performed for T3 by each participant).

In Case I, in order to make sure there is no voluntary effort to suppress tremor during the experiments, all the participants should completely relax their right arm, and the induced tremor generated by an DC motor is suppressed by FES signals instead of muscle torque. The tremor frequency generated by the motor is set to 2Hz in Test 2 ($T_p = 0.5$). The frequency is chosen because the dominant frequency of the typical intention tremor is less than 5Hz [2, 1]. Since Test 2 and Test 3 require the participants performing experiments many times under different controllers, different controller parameters and stimulation input modes, the participants must have enough rest, that is, at least 10 minutes between each test to prevent muscle fatigue [33, 34].

Case II: Experiments on intention tremor patients.

In Case II, two intention tremor patients (No.1: male, 55 years old; No.2: male, 50 years old) were recruited from Rehabilitation Department, Fifth Affiliated Hospital of

Zhengzhou University. The experiment also consists of three test sessions:

T1 : The designated trajectory that patient need to be tracked.

T2 : Voluntary position tracking without FES.

T3 : Voluntary position tracking with FES (2 repeated trials are performed for T3 by the patient).

C. Experimental results

1) Results of parameter identification: The input/output data are used to identify the model components $f_1(u_1)$, $f_2(u_2)$, $G_1(z)$ and $G_2(z)$ using an iterative method. The nonlinear parameters are identified assuming initial linear parameters, and subsequently identifying linear parameters with fixed nonlinear parameters. The nonlinear parameter identification can be readily solved by constrained optimization method solver, e.g. Matlab $fmincon$ function. Then the linear parameters can be easily identified by least square method.

The 1st set of input/output data is used to identify a model and 2nd set of input/output data is used for validating the model. To calculate the fitness of the model, the best fitting value is defined as the percentage,

$$\rho_{\text{fit}} = (1 - \frac{\|y - \hat{y}\|_2}{\|y - \bar{y}\|_2}) \times 100\%, \tag{33}$$

where y is the measured output, $\hat{y}$ denotes the simulated model output. The mean value of y is denoted by $\bar{y}$. In order to reduce the identification computation and design the controller easier, the order of the nonlinear model is selected as $s = 3$ and the orders of linear model are chosen as $n_a = 4$ and $n_b = 2$ respectively. The best fitting value of participant No.1 is 61.26%. The parameter identification best fitting values of the other participants are similar. As a representative example, we can see from Fig. 9 that the simulated outputs are close to the measured output for participant No.1, which verified the effectiveness of the proposed identification method.

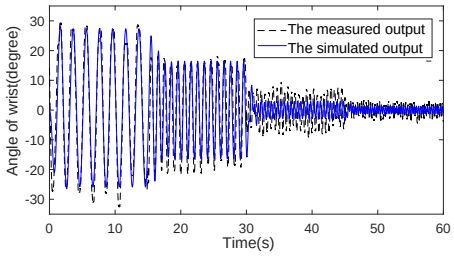

Fig. 9. The simulation and measured output (Participant No.1)

2) Results of wrist tremor suppression: In this subsection, experiments are carried out to compare the performance of the proposed multi-muscle (MM) input mode using FMI-RC algorithm and GB-RC algorithm with the latest design based on single muscle pair (SMP) input mode using these two repetitive control algorithms [25] and the traditional PI high-pass filter (PI-HPF) based algorithm [17] respectively.

During the tests, the sample period T_s is 0.005s. The delay periods of the repetitive controller are $N_p = 100$ with tremor signal $T_p = 0.5$ in Case I and $N_p = 91$ according to the frequency of intention tremor patient in Case II ($T_p = \frac{1}{2.2}$) respectively. The gains of the RC controller are selected as $K_1 = K_2 = 0.5$. Parameters for the order and the cut-off frequency of high-pass Butterworth filter are selected as 6th and 1.2Hz respectively. In order to quantify the performance of different control algorithms on tremor suppression and intuitively analyze the advantages of MM input mode over SMP input mode, the following evaluation indicators are utilized in this paper:

(1) Root mean square error (RMSE)

$$\text{RMSE} = \sqrt{\frac{1}{n}\sum_{i=0}^{n}(y_i - r_i)^2}, \tag{34}$$

where r_i is the designated voluntary reference trajectory (Test 1), y_i is the output of Test 3 and n is the total sample numbers.

(2) Average steady state error (ASSE),

$$\text{ASSE} = \frac{1}{m}\sum_{i=0}^{m}(Y_i - R_i), \tag{35}$$

where R_i is the steady state designated reference trajectory (Test 1), Y_i is the steady state output of Test 3 and m is the sample numbers at last five seconds of each track.

(3) Tremor suppression rate (TSR)

$$\text{TSR} = 1 - \frac{\triangle y}{\triangle v} = 1 - \frac{\sqrt{\frac{1}{n}\sum_{i=0}^{n}(y_i - r_i)^2}}{\sqrt{\frac{1}{n}\sum_{i=0}^{n}(v_i - r_i)^2}}, \tag{36}$$

where $\triangle y$ is the deviation between the output of Test 3 y_i and the designated reference trajectory r_i (Test 1). v_i is the effect of tremor signal on the tracking angles (i.e. without using any controller), which indicates the output of Test 2. $\triangle v$ is the deviation between v_i and r_i.

1. Results-Case I

The experimental results of participant No.1 under different control algorithms with SMP input mode (electrodes attached to FCR and ECR) and MM input mode are shown in Fig. 10 (a), (b) respectively. The tracking results of Test 1 confirms that participants can perform voluntary wrist flexion and extension motion to achieve designated position on the proposed experimental platform. The tracking Test 2 shows the achievement of the voluntary wrist motion under the induced tremor. It can be shown that the tracking Test 3 identify that FES based wrist tremor suppression can attenuate the amplitude of tremor without interference with voluntary wrist motion. As seen in Fig. 10 in particular, the experimental data (T3) from 17 seconds to 18 seconds, the proposed repetitive control algorithms with multi-muscle input mode can attenuate the amplitude of tremor more effectively.

Results of participant No.1 with different control schemes, controller types and controller parameters are shown in Table I, where the values of RMSE and ASSE are given by the mean $\pm$ standard deviation of 5 repeated trials of each task. It can be seen from Table I that the RMSE and ASSE of

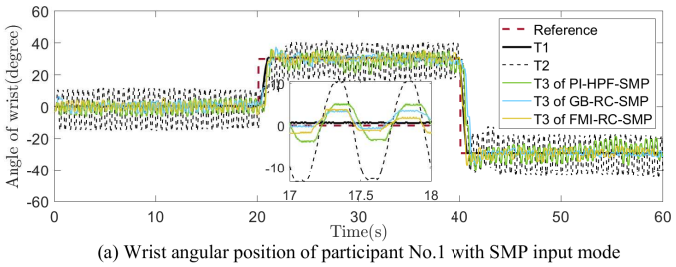

(a) Wrist angular position of participant No.1 with SMP input mode

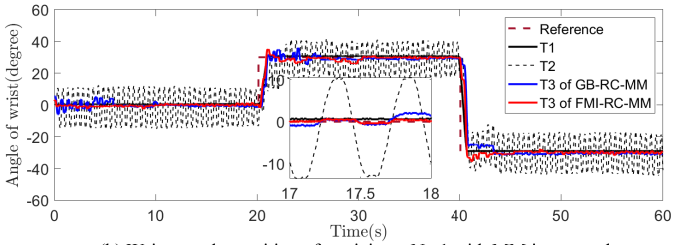

(b) Wrist angular position of participant No.1 with MM input mode

Fig. 10. Wrist angular position of participant No.1 in Case I

FMI-RC algorithm and GB-RC algorithm with multi-muscle input mode are much smaller than the values of PI high-pass filter control algorithm and single muscle pair RC algorithm. The TSR of repetitive controllers with multi-muscle input mode are all obviously higher than single-muscle pair input mode. The maximum TSR of FMI-RC algortihm and GB-RC algorithm with multi-muscle input mode are 87.73% and 83.43% respectively, while the TSR values provided by these two algorithms with single muscle pair input mode are only 78.48% and 78.14%, which verify the advantage of the proposed method. The tracking experimental results of all the other participants (as shown in Table II) also verify the effectiveness of the tremor suppression performance of the proposed control scheme.

TABLE I
STATISTICAL ANALYSIS RESULTS OF PARTICIPANT NO.1

Control Scheme	Controller Type	Controller Parameters	RMSE(°)	ASSE(°)	TSR
SMP	PI-HPF	K_P=20,K_I=20	4.01±0.31	0.59±0.04	52.95%
		K_P=25,K_I=25	4.12±0.26	0.56±0.03	54.04%
		K_P=30,K_I=30	4.03±0.22	0.51±0.04	57.29%
	GB-RC	γ=40	2.50±0.32	0.21±0.04	75.92%
		γ=80	2.29±0.27	0.22±0.03	75.97%
		γ=120	2.09±0.28	0.21±0.03	78.14%
	FMI-RC	m=30,n=24	2.27±0.34	0.21±0.03	77.42%
		m=41,n=36	1.97±0.28	0.21±0.03	77.62%
		m=52,n=47	1.93±0.26	0.20±0.02	78.48%
MM	GB-RC	γ=40	1.52±0.25	0.17±0.02	80.46%
		γ=80	1.51±0.21	0.16±0.02	81.04%
		γ=120	1.42±0.26	0.15±0.02	83.43%
	FMI-RC	m=30,n=24	1.49±0.26	0.14±0.02	83.93%
		m=41,n=36	1.39±0.20	0.13±0.02	84.38%
		m=52,n=47	1.27±0.21	0.10±0.02	87.73%

We further investigate the require FES levels for different control schemes. Due to space reasons, we only provides one detailed experimental results of the FES level of participant No.1, as illustrated in Fig. 11. From Fig. 11 (g-j) and Fig. 11 (a-f), we can see that the FES levels using multi-muscle input mode are much lower than single muscle pair input mode. That means the proposed method can suppress tremor

TABLE II
STATISTICAL ANALYSIS RESULTS OF OTHER PARTICIPANTS

	Control Scheme	Controller Type	Controller Parameters	RMSE(°)	ASSE(°)	TSR
Par-No.2	SMP	PI-HPF	K_P=30,K_I=30	3.42±0.36	0.44±0.03	68.02%
		GB-RC	γ=110	1.52±0.30	0.17±0.03	80.25%
		FMI-RC	m=56,n=42	1.46±0.27	0.14±0.02	85.34%
	MM	GB-RC	γ=110	1.39±0.22	0.12±0.02	86.09%
		FMI-RC	m=56,n=42	0.60±0.18	0.04±0.02	93.72%
Par-No.3	SMP	PI-HPF	K_P=30,K_I=30	4.02±0.51	0.54±0.07	53.19%
		GB-RC	γ=120	3.19±0.43	0.20±0.05	68.49%
		FMI-RC	m=50,n=46	2.34±0.31	0.24±0.03	79.11%
	MM	GB-RC	γ=120	2.39±0.34	0.24±0.04	76.92%
		FMI-RC	m=50,n=46	1.36±0.24	0.17±0.02	85.55%
Par-No.4	SMP	PI-HPF	K_P=30,K_I=30	4.15±0.48	0.56±0.05	58.04%
		GB-RC	γ=115	2.35±0.27	0.22±0.02	75.42%
		FMI-RC	m=52,n=46	1.91±0.37	0.20±0.02	79.94%
	MM	GB-RC	γ=115	1.49±0.21	0.22±0.02	84.32%
		FMI-RC	m=52,n=46	1.09±0.22	0.11±0.01	88.98%

Par: Participant

effectively at lower level of electrical stimulation, and this has the great potential to reduce the possible muscle fatigue. The average extensor and flexor FES levels under different controllers of all the participants are shown in Table III. As shown in Table III, participant No.1's average FES levels of extensor (FES-LE) are 25.89μs with multi-muscle input mode and 136.93μs with single muscle pair input mode. Participant No.1's average FES levels of flexor (FES-LF) with multi-muscle input mode and single muscle pair input mode are 36.17μs and 144.27μs respectively. The average FES levels of extensor and flexor are reduced by 81.09% (reducing from 136.93μs to 25.89μs) and 74.93% (reducing from 144.27μs to 36.17μs) respectively, which means the average FES levels of extensor and flexor muscles with multi-muscle input mode reduced substantially. Moreover, we can see from Table III that compared to the single muscle pair input mode, the average FES-LE and FES-LF of the other three unimpaired participants with multi-muscle input mode decreased by 74.26%, 77.89%, 76.94% and 72.83%, 79.36%, 77.58% respectively.

2. Results-Case II

Representative results with multi-muscle FES input mode for recruited intention tremor patient No.1 in Case II are shown in Fig. 12. T1 is the designated reference trajectory that the patient needs to track. T2 shows tremulous motion trajectory produced by intention tremor patient and the main frequency of Test 2 motion is 2.2Hz. T3 is the wrist motion trajectory after FES based tremor suppression. Fig. 12 shows that the proposed repetitive control algorithms with multi-muscle input mode have better tremor suppression performance than the traditional PI high-pass filter.

The two tremor patients conducts Test 3 twice under the same controller parameters, and final results are averaged. It is shown in Table IV, the FMI-RC and GB-RC with multi-muscle input mode can suppress tremor by up to 82.96% and 81.15% on average respectively. By comparison, PI-HPF algorithm only exhibits an average decrease of 58.06% in tremor amplitude, and the two repetitive control approaches with single muscle pair input mode can suppress tremor less than 70% on average. Meanwhile, as indicated in Table V,

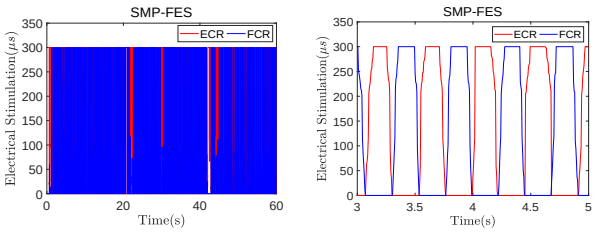

(a) FES level of PI-HPF algorithm with SMP input mode (b) FES level of PI-HPF algorithm with SMP input mode in 3-5 seconds

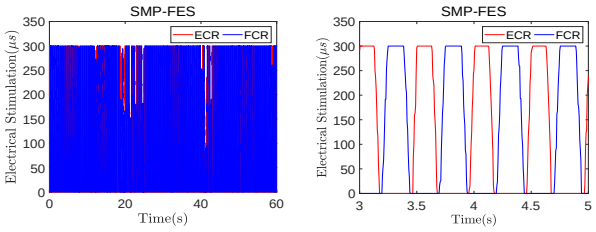

(c) FES level of GB-RC algorithm with SMP input mode (d) FES level of GB-RC algorithm with SMP input mode in 3-5 seconds

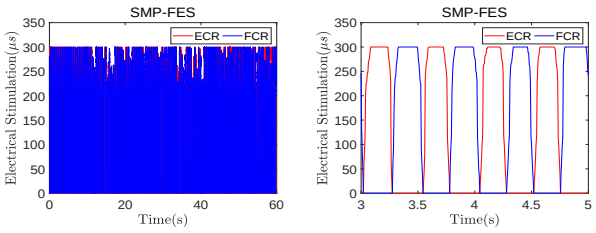

(e) FES level of FMI-RC algorithm with SMP input mode (f) FES level of FMI-RC algorithm with SMP input modein 3-5 seconds

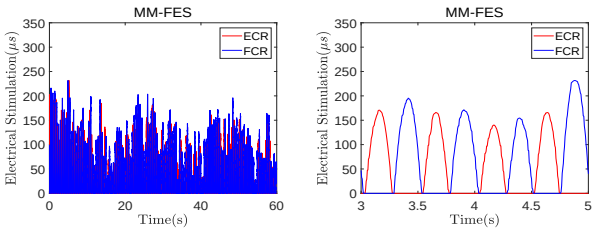

(g) FES level of FMI-RC algorithm with MM input mode (h) FES level of FMI-RC algorithm with MM input mode in 3-5 seconds

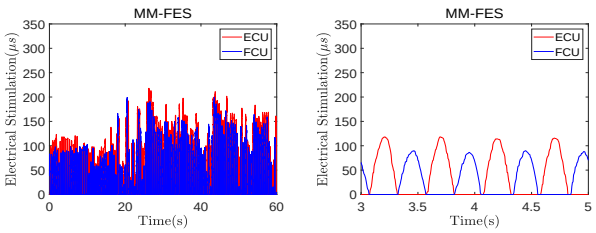

(i) FES level of FMI-RC algorithm with MM input mode (j) FES level of FMI-RC algorithm with MM input mode in 3-5 seconds

Fig. 11. FES levels of different control algorithms with single muscle pair input mode and multi-muscle input mode

the average FES levels with the multi-muscle input mode are much lower than those with single muscle pair input mode. The average FES level of extensor and flexor are reduced by 71.03% and 78.45% respectively.

In order to clearly illustrate the effectiveness of the proposed method, we average all the experimental results

TABLE III
THE AVERAGE FES LEVELS OF EXTENSORS AND FLEXORS

	Control Scheme	Controller Type	Controller Parameters	FES-LE(μs)	FES-LF(μs)
Par-No.1	SMP	PI-HPF	K_P=30,K_I=30	148.12±3.24	151.43±3.11
		GB-RC	γ=120	130.76±2.48	141.25±2.54
		FMI-RC	m=52,n=47	131.91±2.46	140.12±3.67
	MM	GB-RC	γ=120	27.47±1.85	35.28±1.98
		FMI-RC	m=52,n=47	24.30±1.57	37.06±2.57
Par-No.2	SMP	PI-HPF	K_P=30,K_I=30	149.44±3.66	145.70±3.53
		GB-RC	γ=110	141.43±3.34	128.76±2.67
		FMI-RC	m=56,n=42	136.22±3.22	124.26±2.89
	MM	GB-RC	γ=110	36.82±1.98	35.76±1.46
		FMI-RC	m=56,n=42	36.48±2.01	36.47±2.34
Par-No.3	SMP	PI-HPF	K_P=30,K_I=30	150.02±3.03	151.80±3.42
		GB-RC	γ=120	134.23±3.11	124.98±3.02
		FMI-RC	m=50,n=46	132.57±3.24	124.54±3.16
	MM	GB-RC	γ=120	31.43±2.30	27.75±2.18
		FMI-RC	m=50,n=46	30.02±1.98	27.46±2.02
Par-No.4	SMP	PI-HPF	K_P=30,K_I=30	151.02±3.06	146.22±2.97
		GB-RC	γ=115	134.06±2.64	131.78±2.43
		FMI-RC	m=52,n=46	130.24±2.75	127.39±2.84
	MM	GB-RC	γ=115	32.44±2.04	31.10±2.10
		FMI-RC	m=52,n=46	31.41±2.56	29.48±2.23

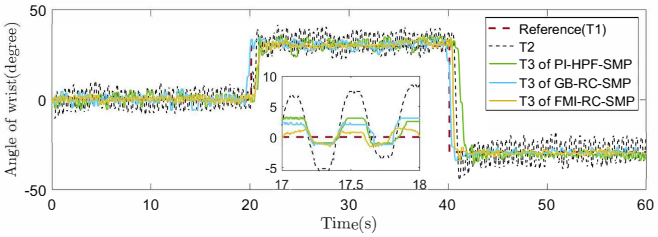

(a) Wrist angular position of patient with SMP input mode

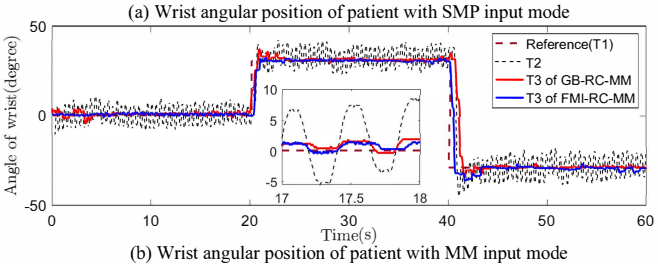

(b) Wrist angular position of patient with MM input mode

Fig. 12. Wrist angular position of intention tremor patient in Case II

TABLE IV
STATISTICAL ANALYSIS RESULTS OF INTENTION TREMOR PATIENTS

	Control Scheme	Controller Type	Controller Parameters	RMSE(°)	ASSE(°)	TSR
Patient No.1	SMP	PI-HPF	K_P=30,K_I=30	4.91±0.66	0.93±0.08	57.80%
		GB-RC	γ=110	2.53±0.37	0.69±0.03	69.54%
		FMI-RC	m=50,n=42	2.39±0.20	0.62±0.03	69.45%
	MM	GB-RC	γ=110	1.73±0.21	0.57±0.02	80.39%
		FMI-RC	m=50,n=42	1.47±0.19	0.55±0.02	81.38%
Patient No.2	SMP	PI-HPF	K_P=30,K_I=30	2.35±0.20	1.35±0.11	58.31%
		GB-RC	γ=120	1.74±0.17	0.53±0.08	70.21%
		FMI-RC	m=52,n=42	1.63±0.21	0.50±0.11	71.22%
	MM	GB-RC	γ=120	0.96±0.16	0.35±0.04	81.90%
		FMI-RC	m=52,n=42	0.93±0.06	0.34±0.04	82.53%

in Case I and Case II. The statistical analysis results of all participants are shown in Fig. 13. As shown in Fig. 13 (a), the TSR values of all participants with multi-muscle input mode are higher than the values with single muscle

TABLE V
THE AVERAGE FES LEVELS OF EXTENSORS AND FLEXORS

	Control Scheme	Controller Type	Controller Parameters	FES-LE(μs)	FES-LF(μs)
Patient No.1	SMP	PI-HPF	K_{P}=30,K_{I}=30	136.02±2.88	115.66±2.63
		GB-RC	γ=110	134.18±2.89	109.02±2.36
		FMI-RC	m=50,n=42	128.84±2.78	110.32±2.54
	MM	GB-RC	γ=110	37.32±2.73	22.76±2.03
		FMI-RC	m=50,n=42	36.02±2.65	19.98±1.34
Patient No.2	SMP	PI-HPF	K_{P}=30,K_{I}=30	135.58±1.93	125.04±2.22
		GB-RC	γ=120	132.26±1.59	120.31±0.68
		FMI-RC	m=52,n=42	124.28±2.11	118.98±1.78
	MM	GB-RC	γ=120	40.15±1.99	29.85±1.31
		FMI-RC	m=52,n=42	39.22±2.35	28.33±1.05

pair input mode. The proposed multi-muscle input mode achieve average 83.92% tremor suppression under repetitive controllers, which is more than 25% higher than the single muscle pair input mode under traditional filter based feedback controller, and about 8% higher than single muscle pair input mode under repetitive controllers. Furthermore, compared with the FES levels of single muscle pair input mode, the average FES levels of extensor and flexor with multi-muscle input mode are substantially reduced. As seen in Fig. 13 (b) and (c), the average FES levels of extensor and flexor of the proposed repetitive controllers with multi-muscle input mode are reduced by 75.43% and 76.82% respectively, which indicates that the proposed method can significantly decrease the FES level and reduce the muscle fatigue.

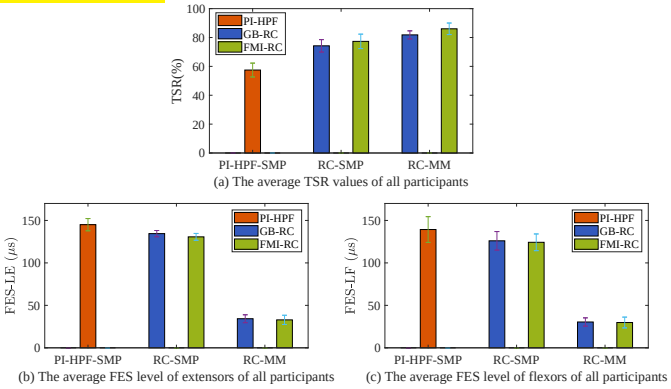

(a) The average TSR values of all participants

(b) The average FES level of extensors of all participants

(c) The average FES level of flexors of all participants

Fig. 13. The statistical analysis results of all participants with SMP and MM input modes

VI. CONCLUSION

This paper consider using multiple muscle FES based RC to suppress wrist intention tremor. To achieve this, a wrist musculoskeletal model with Hammerstein structure is proposed and simplified. Then, a combined linearizing controller and feedback repetitive controller is developed and stability properties are analysed. Two different RC algorithms, FMI-RC algorithm and GB-RC algorithm, are proposed to suppress wrist tremor. Finally, a systematic experimental approach is designed. Both unimpaired participants and intention tremor patient are recruited. The experimental results verify that compared to the existing single muscle pair FES based tremor suppression system, the performance of tremor suppression is enhanced substantially and the average FES levels of extensor and flexor are reduced significantly, which effectively reduces muscle fatigue and improves the comfort of participants.

While the above results are promising, there are some issues that need to be investigated. Firstly, tremor frequency is assumed to be fixed in this paper. However, The frequency of tremor varies with time in reality. The design of adaptive repetitive controller based on frequency variation can obtain better results of tremor suppression and improve the practical application value of the system. Secondly, tremor signal can have multiple-frequency or even a frequency band, therefore proposing multi-periodic RC algorithm can get better performance of tremor suppression, following the latest design for single muscle pair based tremor suppression [35]. Thirdly, there are inevitable model uncertainties associated with the wrist musculoskeletal model, a rigorous analysis and further improvement of the robustness performance of the repetitive controller is also a problem to be considered in future research. Fourthly, the experimental results of healthy participants and intention tremor patient confirm the feasibility and effectiveness of this paper. More testing will be undertaken with intention tremor patients, and the application of the proposed design to other types of tremor patients will be investigated to examine whether the proposed approach is capable to produce significant tremor suppression. Finally, this paper mainly aims to investigate the feasibility of using multiple muscle pair for tremor suppression (designated trajectory tracking). In the future, we will take into account the patients' functional movement as well as the use of non-contact measurement methods. All the above topics are currently been under going and will be reported separately.

REFERENCES

[1] T. A. Saifee. Tremor. *British Medical Bulletin*, 130:51–63, 2019.
[2] K. P. Bhatia, P. Bain, N. Bajaj, et al. Consensus statement on the classification of tremors. From the task force on tremor of the international parkinson and movement disorder society. *Movement Disorders*, 33(1):75–87, 2018.
[3] C. W. Olanow, S. A. Factor, A. J. Espay, et al. Apomorphine sublingual film for off episodes in Parkinson's disease: a randomised, double-blind, placebo-controlled phase 3 study. *The Lancet Neurology*, 19(2):135–144, 2020.
[4] S. S. Raju, A. Niranjan, E. A. Monaco, J. C. Flickinger, and L. D. Lunsford. Stereotactic radiosurgery for medically refractory multiple sclerosis–related tremor. *Journal of Neurosurgery*, 128(4):1214–1221, 2018.
[5] L. Cif and M. Hariz. Seventy years of pallidotomy for movement disorders. *Movement Disorders*, 32(7):972–982, 2017.
[6] K. P. Michmizos, B. Lindqvist, S. Wong, E. L. Hargreaves, K. Psychas, G. D. Mitsis, S. F. Danish, and K. S. Nikita. Computational neuromodulation: Future challenges for deep brain stimulation. *IEEE Signal Processing Magazine*, 34(2):114–119, 2017.
[7] F. Hawes, C. Billups, and S. Forwell. Interventions for upper-limb intention tremor in multiple sclerosis. *International Journal of MS Care*, 12(3):122–132, 2010.
[8] P. Feys, W. Helsen, X. Liu, D. Mooren, H. Albrecht, B. Nuttin, and P. Ketelaer. Effects of peripheral cooling on intention tremor in multiple sclerosis. *Journal of Neurology, Neurosurgery & Psychiatry*, 76(3):373–379, 2005.
[9] D. Case, B. Taheri, and E. Richer. A lumped-parameter model for adaptive dynamic MR damper control. *IEEE/ASME Transactions on Mechatronics*, 20(4):1689–1696, 2015.
[10] C. R. Kelley and J. L. Kauffman. Tremor-active controller for dielectric elastomer-based pathological tremor suppression. *IEEE/ASME Transactions on Mechatronics*, 25(2):1143–1148, 2020.
[11] A. Prochazka, J. Elek, and M. Javidan. Attenuation of pathological tremors by functional electrical stimulation I: Method. *Annals of Biomedical Engineering*, 20(2):205–224, 1992.
[12] A. P. L. Bó, P. Poignet, and C. Geny. Filtering voluntary motion for pathological tremor compensation. In *2009 IEEE/RSJ International Conference on Intelligent Robots and Systems*, pages 55–60. IEEE, 2009.

[13] A. P. L. Bó and P. Poignet. Tremor attenuation using FES-based joint stiffness control. In *2010 IEEE International Conference on Robotics and Automation*, pages 2928–2933. IEEE, 2010.
[14] D. Zhang, P. Poignet, F. Widjaja, and T. A. Wei. Neural oscillator based control for pathological tremor suppression via functional electrical stimulation. *Control Engineering Practice*, 19(1):74–88, 2011.
[15] E. H. Copur, C. T. Freeman, B. Chu, and D. S. Laila. Repetitive control of electrical stimulation for tremor suppression. *IEEE Transactions on Control Systems Technology*, 27(2):540–552, 2019.
[16] C.S. To, R. Kobetic, J. R. Schnellenberger, M. L. Audu, and R. J. Triolo. Design of a variable constraint hip mechanism for a hybrid neuroprosthesis to restore gait after spinal cord injury. *IEEE/ASME Transactions on Mechatronics*, 13(2):197–205, 2008.
[17] M. Javidan, J. Elek, and A. Prochazka. Attenuation of pathological tremors by functional electrical stimulation II: clinical evaluation. *Annals of Biomedical Engineering*, 20(2):225–236, 1992.
[18] J. W. Ramsay, B. V. Hunter, and R. V. Gonzalez. Muscle moment arm and normalized moment contributions as reference data for musculoskeletal elbow and wrist joint models. *Journal of Biomechanics*, 42(4):463–473, 2009.
[19] A. J. Buckmire, T. J. Arakeri, J. P. Reinhard, and A. J. Fuglevand. Mitigation of excessive fatigue associated with functional electrical stimulation. *Journal of Neural Engineering*, 15(6):066004, 2018.
[20] S. L. Delp, F. C. Anderson, A. S. Arnold, P. Loan, A. Habib, C. T. John, E. Guendelman, and D. G. Thelen. Opensim: open-source software to create and analyze dynamic simulations of movement. *IEEE Transactions on Biomedical Engineering*, 54(11):1940–1950, 2007.
[21] S. Sakariya, C. T. Freeman, and K. Yang. Iterative learning control of functional electrical stimulation in the presence of voluntary user effort. *Control Engineering Practice*, 96:1–11, 2020.
[22] F. Le, I. Markovsky, C.T. Freeman, and E. Rogers. Identification of electrically stimulated muscle models of stroke patients. *Control Engineering Practice*, 18(4):396–407, 2010.
[23] J. A. Gallego, J. L. Dideriksen, A. Holobar, J. Ibáñez, V. Glaser, J. P. Romero, J. Benito-León, J. Pons, E. Rocon, and D. Farina. The phase difference between neural drives to antagonist muscles in essential tremor is associated with the relative strength of supraspinal and afferent input. *Journal of Neuroscience*, 35(23):8925–8937, 2015.
[24] W. K. Durfee and K. E. Maclean. Methods for estimating isometric recruitment curves of electrically stimulated muscle. *IEEE Transactions on Biomedical Engineering*, 36(7):654–667, 1989.
[25] C. T. Freeman, P. Sampsonb, J. H. Burridgeb, and A. M. Hughesb. Repetitive control of functional electrical stimulation for induced tremor suppression. *Mechatroics*, 32:79–87, 2015.
[26] G. M. Lyons, G. E. Leane, M. M. Clarke, J. V. O'brien, and P. A. Grace. An investigation of the effect of electrode size and electrode location on comfort during stimulation of the gastrocnemius muscle. *Medical Engineering & Physics*, 26(10):873–878, 2004.
[27] F. M. Colacino, R. Emiliano, and B. R. Mace. Subject-specific musculoskeletal parameters of wrist flexors and extensors estimated by an EMG-driven musculoskeletal model. *Medical Engineering & Physics*, 34(5):531–540, 2012.
[28] M. Curtin and M. M Lowery. Musculoskeletal modelling of muscle activation and applied external forces for the correction of scoliosis. *Journal of Neuroengineering and Rehabilitation*, 11(1):52, 2014.
[29] S. Takehara, M. Murakami, and K. Hase. Biomechanical evaluation of an electric power-assisted bicycle by a musculoskeletal model. *Journal of System Design and Dynamics*, 6(3):343–350, 2012.
[30] V. H. Duenas, C. A. Cousin, A. Parikh, P. Freeborn, E. J. Fox, and W. E. Dixon. Motorized and functional electrical stimulation induced cycling via switched repetitive learning control. *IEEE Transactions on Control Systems Technology*, 27(4):1468–1479, 2018.
[31] R. W. Longman. On the theory and design of linear repetitive control systemsg. *European Journal of Control*, 16(5):447–496, 2010.
[32] J. J. Hätönen, C.T. Freeman, D.H. Owens, P. L. Lewin, and E. Rogers. A gradient-based repetitive control algorithm combining ILC and pole placement. *European Journal of Control*, 12(3):278–292, 2006.
[33] Q. Zhang, M. Hayashibe, P. Fraisse, and D. Guiraud. FES-induced torque prediction with evoked emg sensing for muscle fatigue tracking. *IEEE/ASME Transactions on Mechatronics*, 16(5):816–826, 2011.
[34] M. Vromans and P. D. Faghri. Functional electrical stimulation-induced muscular fatigue: Effect of fiber composition and stimulation frequency on rate of fatigue development. *Journal of Electromyography and Kinesiology*, 38:67–72, 2018.
[35] Z. Zhang, B. Chu, Y. Liu, and D. H. Owens. FES based wrist tremor suppression using multi-periodic repetitive control. *IFAC-PapersOnLine*, 53(2):10135–10140, 2020.

Zan Zhang received the B.E. and M.E. degrees in college of electrical and information engineering from Hunan University, Changsha, China, in 2002 and 2005 respectively. Since 2017, she has been a doctoral student with Zhengzhou University.

She is currently a lecturer with the School of Electrical Engineering, Zhengzhou University. Her research interests include repetitive control, active disturbance rejection control, and their applications in biomedical engineering and rehabilitation robots.

Bing Chu received the B.E. degree and the M.E. degree from Tsinghua University, Beijing, China, in 2004 and 2007, respectively, and the Ph.D. degree from The University of Sheffield, Sheffield, U.K., in 2009. He was a Post-Doctoral Researcher with the University of Oxford, Oxford, U.K., from 2010 to 2012.

He is currently an Associate Professor in Electronics and Computer Science with the University of Southampton, Southampton, U.K. His current research interests include iterative learning and repetitive control, applied optimization theory, and their applications to robotics, power electronics, and next generation healthcare.

Yanhong Liu received the B.E. degree from the Zhengzhou University of Light Industry, Zhengzhou, China, in 1992, and the M.E. and Ph.D. degrees from Tsinghua University, Beijing, China, in 2002 and 2006, respectively. From 2012 to 2013, she was a Visiting Scholar with the University of California at San Diego, San Diego, USA.

She is currently a Professor with the School of Electrical Engineering, Zhengzhou University. Her current research interests include nonlinear system modelling and control, robotic control, and human-robot interactions and collaborations.

Zhe Li received his B.M. and M.M. degree from Henan University of Chinese Medicine, Zhengzhou, China, in 1996 and 2000 respectively. He received his Ph.D degree in Rehabilitation Medicine and Physiotherapy from Huazhong University of Science and Technology, Wuhan, China, in 2010.

He is currently a Senior Doctor with the Rehabilitation Department of the Fifth Affiliated Hospital of Zhengzhou University. His research interest is the basic and clinical research on nerve rehabilitation.

David H Owens received the B.Sc. and ARCS degrees in physics in 1969 and the Ph.D. degree in control engineering in 1973, both from Imperial College, London, U.K.

He is currently a Professor with the School of Electrical Engineering, Zhengzhou University. He is also with Department of Automatic Control and Systems Engineering, the University of Sheffield. His current research interests includes the robust optimization-based iterative learning control, repetitive control and their applications in mechanical systems, rehabilitation robotics and manufacture.